Development 134, 4033-4041 (2007) doi:10.1242/dev.009167

FGF signaling acts upstream of the NOTCH and WNT signaling pathways to control segmentation clock oscillations in mouse somitogenesis

Matthias B. Wahl[1], Chuxia Deng[2], Mark Lewandoski[3] and Olivier Pourquié[1,4,*]

Fibroblast growth factor (FGF) signaling plays a crucial role in vertebrate segmentation. The FGF pathway establishes a posterior-to-anterior signaling gradient in the presomitic mesoderm (PSM), which controls cell maturation and is involved in the positioning of segmental boundaries. In addition, FGF signaling was shown to be rhythmically activated in the PSM in response to the segmentation clock. Here, we show that conditional deletion of the FGF receptor gene *Fgfr1* abolishes FGF signaling in the mouse PSM, resulting in an arrest of the dynamic cyclic gene expression and ultimately leading to an arrest of segmentation. Pharmacological treatments disrupting FGF signaling in the PSM result in an immediate arrest of periodic WNT activation, whereas NOTCH-dependent oscillations stop only during the next oscillatory cycle. Together, these experiments provide genetic evidence for the role of FGF signaling in segmentation, and identify a signaling hierarchy controlling clock oscillations downstream of FGF signaling in the mouse.

KEY WORDS: FGF, Somite, Segmentation, Clock, Oscillation, Vertebra

INTRODUCTION

The striking segmented pattern of the human spine is established during embryogenesis when somites are rhythmically added to the forming posterior part of the embryo. Current models of somitogenesis are based on the clock and wavefront model in which a temporal periodicity generated by the clock in presomitic mesoderm (PSM) cells is translated into the periodic array of somites at the wavefront level (Cooke and Zeeman, 1976; Pourquie, 2003). In the mouse, the clock is a molecular oscillator driving periodic pulses of notch, fibroblast growth factor (FGF) and Wnt signaling in the PSM, with a periodicity matching that of somite production (Aulehla et al., 2003; Dequeant et al., 2006; Palmeirim et al., 1997). The wavefront has been shown to involve a posterior gradient of Wnt and FGF/MAPK activity opposed to a retinoic acid (RA) gradient, which regresses posteriorly in concert with the formation of posterior structures (Aulehla et al., 2003; Diez del Corral and Storey, 2004; Dubrulle et al., 2001; Dubrulle and Pourquie, 2004b; Sawada et al., 2001). This traveling gradient defines a threshold of FGF signaling (the determination front) in the PSM, below which cells become competent to respond to the clock signal (Dubrulle and Pourquie, 2004a). When cells reach the anterior PSM, the FGF-mediated repression is relieved, allowing activation of genes controlling the segmentation program, such as *Mesp2*, in response to the clock signal (Delfini et al., 2005). In this model, the size of a segment depends on the distance traveled by the wavefront during one oscillation cycle. Therefore, interference with the FGF gradient results in modification of somite size (Diez del Corral et al., 2003; Dubrulle et al., 2001; Sawada et al., 2001; Vermot and Pourquie, 2005). Thus far, this model is based essentially on gain-of-function experiments or pharmacological blockade of the FGF/MAPK pathway in chick, frog and fish (Diez del Corral et al., 2003; Dubrulle et al., 2001; Sawada et al., 2001; Vermot and Pourquie, 2005). No direct genetic evidence for the clock and wavefront model has been provided, partly due to the fact that the FGF pathway is required during gastrulation. Thus, null mutation of genes, such as *Fgf8* or *Fgfr1* in the mouse, results in a severe gastrulation defect and the quasi absence of paraxial mesoderm, thus precluding studies of the segmentation process (Deng et al., 1994; Sun et al., 1999). Here, we analyze the effect of a conditional deletion in the mesoderm of *Fgfr1*, the only FGF receptor expressed in the mouse paraxial mesoderm. We show that this mutation disrupts normal cyclic gene expression in the PSM and results in abnormal segmentation of somites and vertebrae. Also, we observe that inhibition of the FGF/MAPK pathway in cultured mouse embryos blocks oscillations of the *Wnt* and *Notch* cyclic genes with different kinetics. These experiments provide genetic evidence for the role of FGF signaling in positioning the determination front in mouse, and suggest that FGF acts upstream of the Wnt and Notch pathways to control the segmentation clock oscillations.

MATERIALS AND METHODS

Generation of mutant embryos

Males carrying one conditional allele for *Fgfr1* (*Fgfr1*$^{f/+}$) (Xu et al., 2002) and positive for the *T-Cre* transgene (Perantoni et al., 2005) (both on a C57BL/6 genetic background) were mated to homozygous floxed *Fgfr1* females (*Fgfr1*$^{f/f}$) in order to generate *Fgfr1*$^{f/f}$*;T-Cre* progeny. To analyze the status of RA signaling, mice were crossed to the *RARE* (also known as *Rare1* – Mouse Genome Informatics)-*lacZ* mice (Rossant et al., 1991) and β-gal staining was performed using X-Gal as substrate. The floxed *Fgfr1* allele was genotyped using primer F: CTGGTATCCT-GTGCCTATC and primer R: CAATCTGAT CCCAAGACCAC; *T-Cre* using primer F: CCTCATCCCGATCTCGGTGCTCCTT and primer R: GCCTGGCGATCCCTGAACATGTCCA; and *RARE-lacZ* mice using primer F: TGGCGTTACCCAACTTAATCG and primer R: ACGAG-GACAGTATCGGCCTC.

[1]Stowers Institute for Medical Research, Kansas City, MO 64110, USA. [2]Genetics of Development and Diseases Branch, National Institutes of Diabetes and Digestive and Kidney Diseases, National Institutes of Health, Bethesda, MD 20892, USA. [3]Laboratory of Cancer and Developmental Biology, NCI-Frederick, National Institutes of Health, Frederick, MD 21702, USA. [4]Howard Hughes Medical Institute, Kansas City, MO 64110, USA.

*Author for correspondence (e-mail: olp@stowers-institute.org)

Accepted 23 August 2007

Mouse tail culture

E9.5 embryo tails were cultured in 10% FBS in DMEM-F12 or 50% rat serum in DMEM-F12 at 37°C in 5% CO_2 (Correia and Conlon, 2000) either in 0.1% DMSO or in the presence of the pharmaceutical inhibitors U0126, 100 μM (Promega) or SU5402, 100 μM (Pfizer) in 0.1% DMSO. Explants were cultured for periods ranging from 1-6 hours and were then fixed in 4% formaldehyde and processed for in situ hybridization.

Real-time PCR

RNA from the posterior region of E8.5 mouse tails at the 5- to 9-somite stage was extracted using Trizol reagent (Invitrogen). Embryos were cut in the middle of the PSM and the posterior part was used for RNA isolation and the remaining embryo was subject to genotyping. cDNA was synthesized using SuperScript II (Invitrogen) and for each gene, three independent real-time PCR reactions (each in duplicate) were performed using TaqMan (7900 Fast System, Applied Biosystems) with probes for *Hprt* (Mm01545399_m1), *Erm* (Mm00465816_m1) and *Pea3* (Mm00465816_m1).

Skeletal examination

Preparation of skeletons and staining with Alizarin Red (bone) and Alcian Blue (cartilage) were performed as described previously (Kessel et al., 1990).

In situ hybridization

In situ hybridization was performed as described previously (Henrique et al., 1995). All probes for in situ hybridization were either amplified by RT-PCR [*Fgfr1* (primer F: ATGCACTCCCATCCTCGGAA, primer R: GGATCTGGACATACGGCAAG and primer F: GGTCTTAGGCAAACCACTTG, primer R: CCTAAACAGAAACCTCACGG); *Msgn1* (primer F: ATGGACAACCTGGGTGAGAC, primer R: TCACACACTCTGTGGCCTGG); *Paraxis* (primer F: TGCTGAGCGAGGACGAGGAGAA, primer R: CCTCCCCGATTTGCTCACAT); *Raldh2* (primer F: ACTCAGAGAGTGGGAGAGTG, primer R: AATGAAGAAGCCCTTCCTTC); *Sox2* (primer F: CCCAGCGCCCGCATGTATAA, primer R: TCCCCTTCTCCAGTTCGCAG); *Spry2* (primer F: GGAAAGAAGGAAAAAGTTTGCATCA, primer R: TTTTTACAACGACAACCCGG); *Sef* (primer F: CAGGAACAGCGGACTGCACA; primer R: GCCACAGAAATCTTGCAGGA)] or have been previously described in the literature (*Axin2, Cyp26*, *Dkk1*-intronic, *Dll1*, *Dll3*, *Dusp6*, *Erm*, *Fgf3*, *Fgf4*, *Fgf8*, *Fgf17*, *Gbx2*, *Lfng*, *Lfng*-intronic, *Mesp2*, *Notch1*, *Pea3*, *Shh*, *Snail1*, *T*, *Uncx4.1*, *Wnt3a*). Mouse Genome Informatics lists some of the above genes with different names and symbols; they are, *Paraxis* as *Tcf15*, *Raldh2* as *Aldh1a2*, *Sef* as *Il17rd*, *Cyp26* as *Cyp26a1*, *Erm* as *Etv5* and *Pea3* as *Etv3.*

RESULTS

Conditional deletion of *Fgfr1* in the paraxial mesoderm disrupts segmentation

A difficulty in genetically studying FGF loss of function is the high redundancy of FGF pathway members. For example, the genes coding for the FGF ligands *Fgf3*, *Fgf4*, *Fgf8* and *Fgf17*, are expressed in the mouse PSM or its precursors in the primitive streak and tail bud (Crossley and Martin, 1995; Mansour et al., 1993; Maruoka et al., 1998; Niswander and Martin, 1992). Accordingly, conditional deletion of *Fgf8* in the primitive streak and/or PSM does not lead to a segmentation phenotype, suggesting that these other ligands might act redundantly in this process (Perantoni et al., 2005). Here, we have carefully compared the expression of *Fgf3, Fgf4* and *Fgf17* to that of *Fgf8* in the mouse PSM (Fig. 1A-D). We observed that only *Fgf4* is not expressed in a gradient in the posterior PSM (Fig. 1B). *Fgf4* expression is restricted to a small cell population in the tail bud, which also expresses the other FGF ligands. By contrast, *Fgfr1* is the only known FGF receptor we could detect by in situ hybridization in the PSM (Fig. 1E). Since mice homozygous for a null *Fgfr1* allele do not form PSM or somites because of a

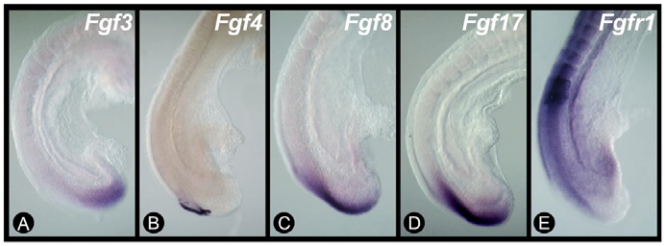

Fig. 1. Expression of *Fgf* ligands. In situ hybridization for (**A**) *Fgf3*, (**B**) *Fgf4*, (**C**) *Fgf8*, (**D**) *Fgf17* and (**E**) *Fgfr1,* in E9.0 embryos. *Fgf3*, *Fgf8* and *Fgf17* are expressed in a gradient in the posterior PSM. *Fgf4* expression is restricted to a small cell population in the tail bud, which also expresses the other FGF ligands.

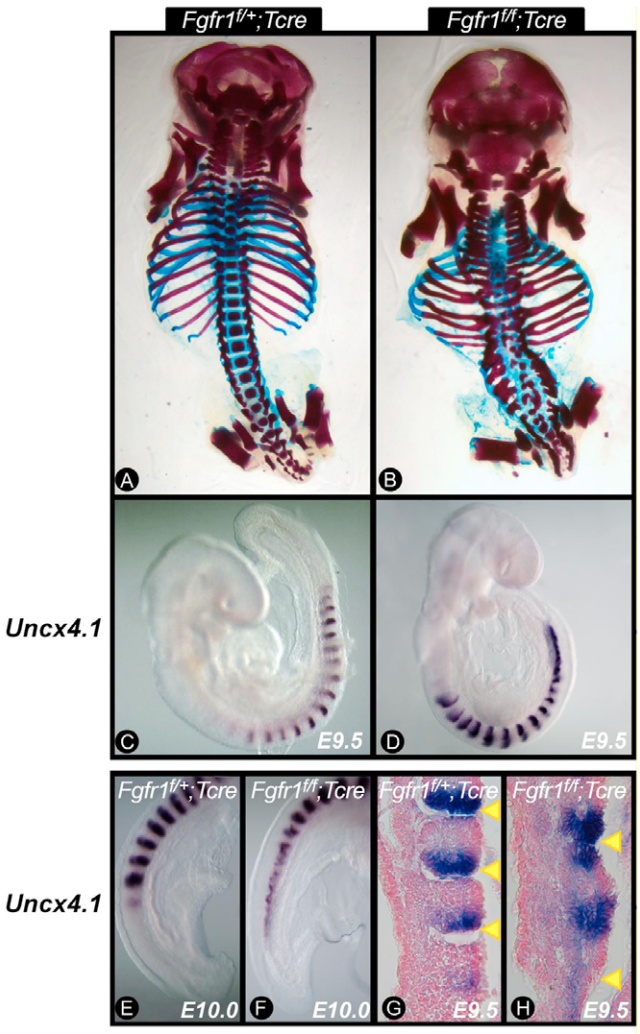

Fig. 2. Progressive disruption of segmentation in the *Fgfr1$^{f/f}$;T-Cre* mutant embryos. (**A**,**B**) Skeletons stained with Alizarin Red (bone) and Alcian Blue (cartilage). (**C-H**) *Uncx4.1* staining in *Fgfr1$^{f/+}$;T-Cre* control (C,E,G) and *Fgfr1$^{f/f}$;T-Cre* mutant embryos (D,F,H); C and D show whole mounts of E9.5 embryos and E and F are higher magnifications of the somite region at E10.0. (G,H) Sagittal sections through *Uncx4.1*-stained embryos. The posterior-most *Uncx4.1*-positive region is shown at the same magnification for both. In the *Fgfr1$^{f/f}$;T-Cre* mutant embryos (H), somites fail to separate and a giant somite spanning over the region normally covering two somites is formed. Arrowheads indicate the boundaries between somites.

gastrulation defect (Deng et al., 1994), we used a conditional *Fgfr1* allele in which exons 9-13 are flanked by LoxP sites (Xu et al., 2002). This mouse line was crossed to the *T-Cre* line in which *Cre* is controlled by the *T* primitive streak enhancer, which promotes recombination in most primitive streak descendants including somites, PSM and tail bud (data not shown) (Perantoni et al., 2005). Fetuses homozygous for the floxed allele of *Fgfr1* and positive for the *T-Cre* transgene (hereafter called *Fgfr1$^{f/f}$;T-Cre*) survive up to birth, but die neonatally. Skeletal preparations from *Fgfr1$^{f/f}$;T-Cre* fetuses and neonates clearly showed, in all specimens, axial truncations in the sacral and tail regions, whereas the anterior segments were formed (Fig. 2A,B). We also observed rudimentary hind limbs as previously reported (data not shown) (Verheyden et al., 2005). Although cervical vertebrae appeared to be normal, more posteriorly, vertebrae and ribs became progressively fused (Fig. 2B and data not shown). Irregular skeletal elements corresponding to fused lumbar and sacral vertebral elements were present, but the caudal region did not form. These observations are consistent with a progressive disruption of the segmentation process in *Fgfr1$^{f/f}$;T-Cre* mutants.

To trace the origin of these defects, we analyzed segmentation in detail in mutant embryos between E8.5 and E10.5. Somite formation was first examined using the *Uncx4.1* probe which marks the posterior compartment of formed somites (Mansouri et al., 1997). Whereas approximately the first 10-13 somites appeared relatively normal in the mutant embryos (Fig. 2C-F and data not shown), larger irregular somites were often seen in *Fgfr1$^{f/f}$;T-Cre* embryos at the level of somites 10-15 (n=6/6; Fig. 2G,H, arrowheads). Surprisingly, *Uncx4.1* expression was not always found in the posterior compartment of these larger somites (Fig. 2H). Posterior to this region, no clear segmented structures were observed (Fig. 2D,F and data not shown), and the region appeared abnormal, with an enlarged neural tube expressing *Sox2* and a thinner PSM (Fig. 3A,B and data not shown). *Shh* expression was weaker, but nevertheless detected

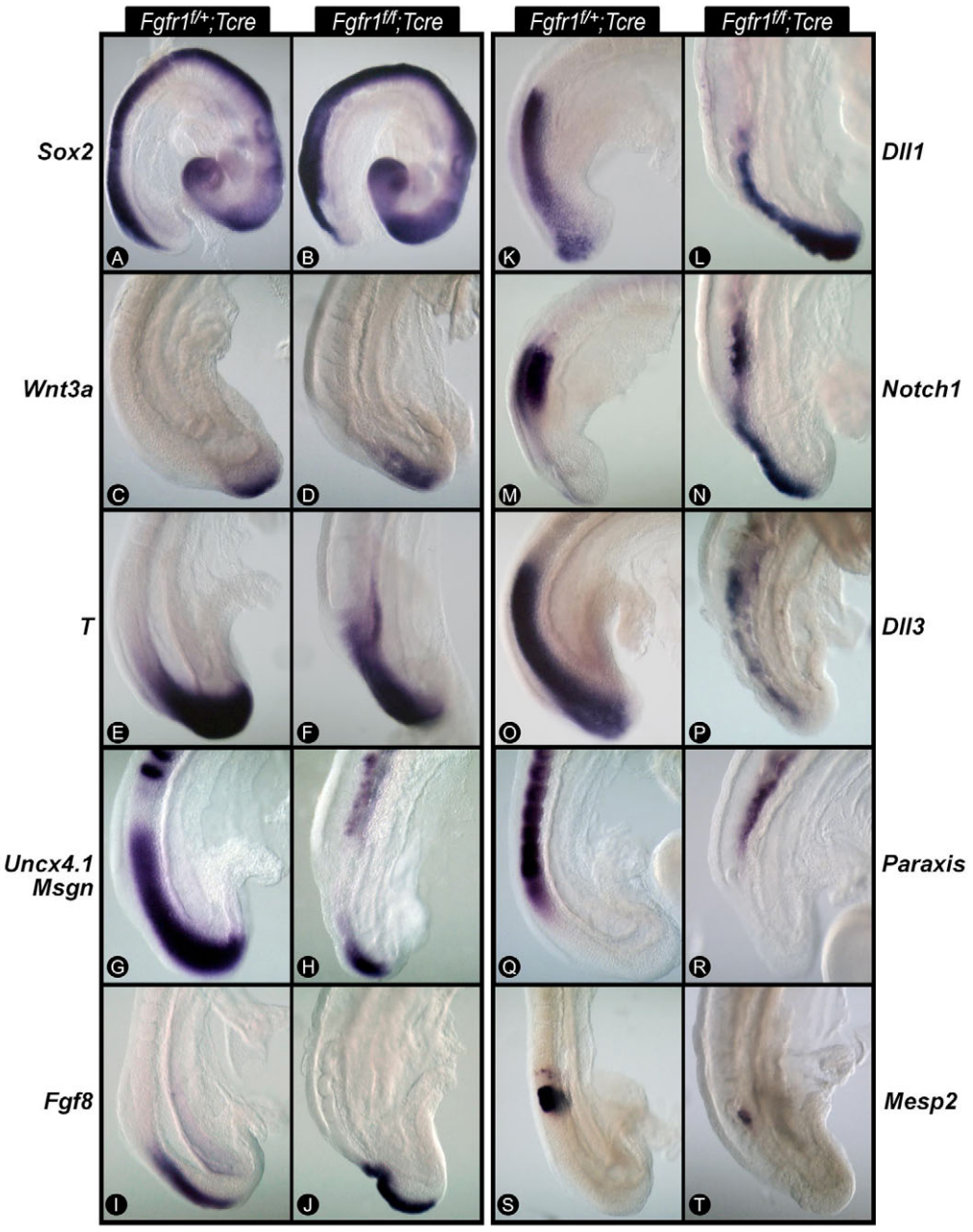

Fig. 3. Expression of different marker genes in E9.0 *Fgfr1$^{f/f}$;T-Cre* mutant embryos. Expression of (**A**,**B**) *Sox2*, (**C**,**D**) *Wnt3a*, (**E**,**F**) *T*, (**G**,**H**) *Uncx4.1/Msgn1*, (**I**,**J**) *Fgf8*, (**K**,**L**) *Dll1*, (**M**,**N**) *Notch1*, (**O**,**P**) *Dll3*, (**Q**,**R**) *Paraxis* and (**S**,**T**) *Mesp2* in *Fgfr1$^{f/+}$;T-Cre* control and *Fgfr1$^{f/f}$;T-Cre* mutant embryos, respectively.

all along the notochord and the floor plate, suggesting a normal differentiation of axial structures (data not shown). *Wnt3a* expression was maintained in the tail bud (Fig. 3C,D), and its downstream targets involved in PSM patterning, including *T* (Fig. 3E,F), *Msgn1* (Fig. 3G,H), *Fgf8* (Fig. 3I,J) and *Dll1* (Fig. 3K,L) were expressed in the posterior PSM. The expression domain of *Msgn1* was, nevertheless, much smaller than in wild-type embryos and was confined to the posterior-most region of the PSM (Fig. 3G,H). *Dll1* is normally expressed in an anterior-to-posterior gradient in the PSM (Fig. 3K) but in the mutant embryos, the expression gradient was reversed, with the strongest expression found in the tail bud (Fig. 3L), suggesting that FGF represses *Dll1* transcription. *Mesp2*, which marks the future segment territory at the determination front level was severely downregulated in the region failing to form somites in the mutants (Fig. 3S,T). Interestingly, the somitic marker *Uncx4.1* is nevertheless expressed in the posterior unsegmented region, indicating that paraxial mesoderm maturation still proceeds in the absence of somite formation (Fig. 2D,F).

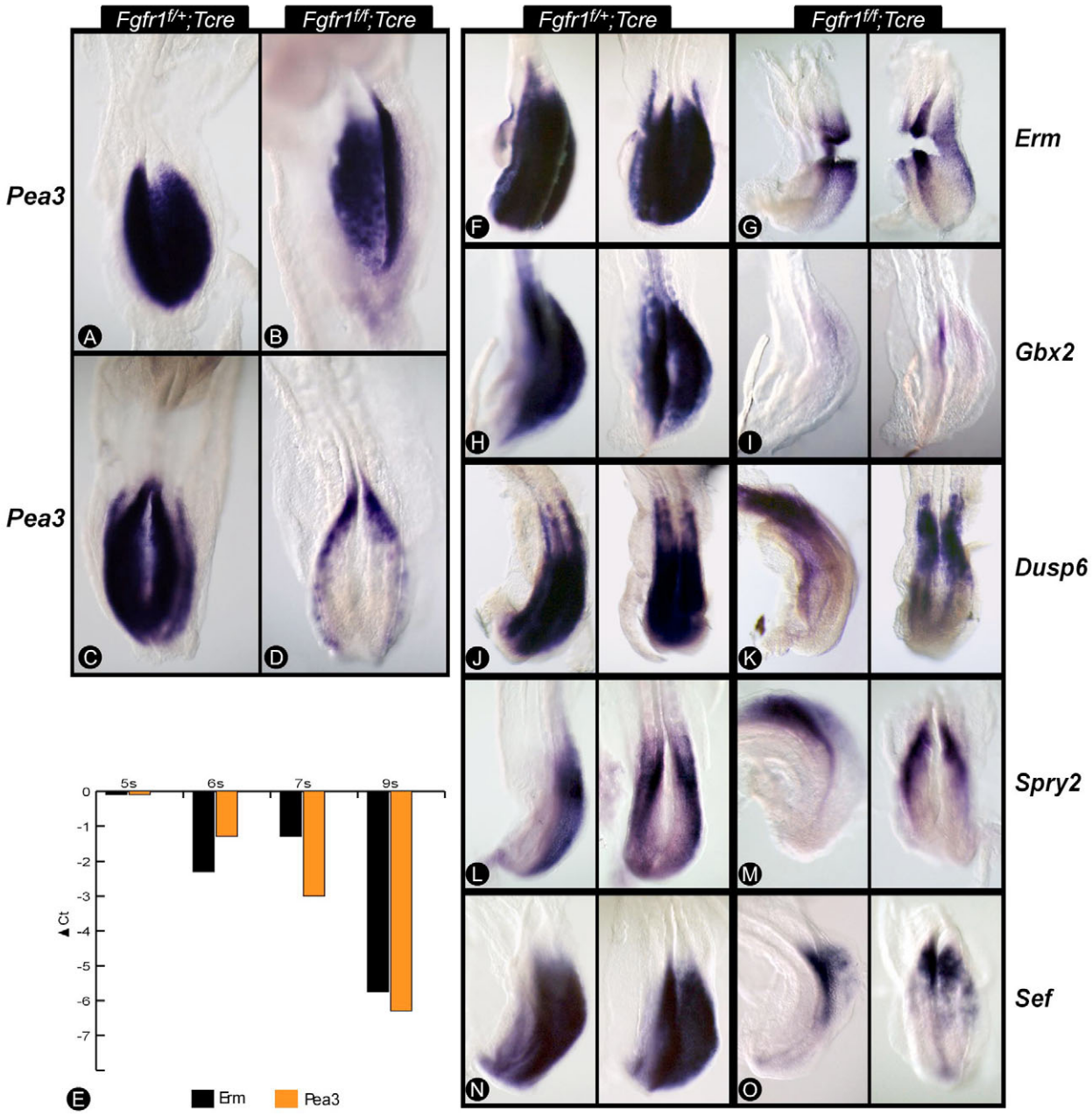

Fig. 4. Progressive downregulation of FGF target genes in *Fgfr1$^{f/f}$;T-Cre* mutant embryos after the 6-somite stage. (**A-D**) *Pea3* is normally expressed in control (A) and *Fgfr1$^{f/f}$;T-Cre* (B) embryos at the 5-somite stage, and in 7-somite control embryos (C), but it becomes progressively downregulated in the posterior PSM/tail bud of 7-somite *Fgfr1$^{f/f}$;T-Cre* mutant embryos (D). (**E**) Real-time PCR for FGF target genes *Erm* and *Pea3* in the posterior tail of *Fgfr1$^{f/f}$;T-Cre* mutant embryos and *Fgfr1$^{f/+}$;T-Cre* control embryos at somite stages 5 (n=1/1), 6 (n=3/5), 7 (n=2/2) and 9 (n=1/1). Both genes become progressively downregulated from somite stages 6 onward. Levels of *Erm* and *Pea3* were normalized to the housekeeping gene *Hprt* and values are given as the mean change in crossing points (C_T) in *Fgfr1$^{f/f}$; T-Cre* mutant embryos. (**F-O**) For other target genes (F,G) *Erm*, (H,I) *Gbx2*, (J,K) *Dusp6*, (L,M) *Spry2* and (N,O) *Sef*, the expression in the posterior PSM and the tail bud of E8.75 *Fgfr1$^{f/f}$;T-Cre* mutant embryos is lost, whereas the expression in the anterior PSM and the adjacent structures is normal.

To relate the somitogenesis defect to FGF activation, we first carefully mapped the timing of loss of FGF signaling in the conditional mutants by in situ hybridization for the known FGF target *Pea3* (Fig. 4A-D) (Chotteau-Lelievre et al., 2001). Between the 5- to 7-somite stage, the expression level of *Pea3* became strongly downregulated in the posterior PSM and tail bud, suggesting that FGF signaling in the posterior paraxial mesoderm begins to decrease around this time (Fig. 4A-D and data not shown). To confirm this, we analyzed the expression levels of the two FGF target genes *Pea3* and *Erm* in the posterior embryo, including the posterior PSM and the tail bud, by quantitative real-time PCR. Expression of these genes decreased progressively from the 5-somite stage onward (Fig. 4E). We also analyzed the expression of other known FGF target genes including *Erm*, *Gbx2*, *Dusp6*, *Spry2* and *Sef* by in situ hybridization and observed that they are also downregulated in the posterior PSM and tail bud of *Fgfr1$^{f/f}$;T-Cre* embryos after the 5- to 8-somite stage (Fig. 4F-O). Together, this suggests that FGF signaling becomes progressively downregulated in the paraxial mesoderm posterior to somite 5, approximately. These observations indicate that the progressive failure of somite boundary formation in these mutants parallels the progressive loss of FGF signaling in the forming PSM.

Loss of FGF signaling does not alter the positioning of the RA-responsive domain in the PSM but disrupts cyclic gene oscillations

The posterior FGF signaling gradient has been shown to be antagonized by an opposing RA gradient resulting from the production of RA by its biosynthetic enzyme RALDH2 in the segmented region of the embryo (Diez del Corral et al., 2003). In *Fgfr1$^{f/f}$;T-Cre* embryos, expression of the transcript for the RA-degrading enzyme Cyp26 that is normally found in the tail bud region, is strongly downregulated (Fig. 5A,B). This is expected to lead to a gain of function of RA signaling and hence, a posterior extension of the RA-responsive domain. However, no significant difference in the positioning of the RA-responsive domain was detected between the wild-type and mutant mice using the *RARE-lacZ* mouse reporter (Rossant et al., 1991) (Fig. 5C,D). Consistently, expression of genes normally expressed in the RA-responsive domain, such as *Paraxis* (Fig. 3Q,R) or *Raldh2* (Fig. 5E,F) was not significantly disrupted in the *Fgfr1$^{f/f}$;T-Cre* embryos. A progressive shrinking of the *Msgn1*-positive, *Uncx4.1*-negative domain in the posterior PSM is nevertheless observed after the E9.5-somite stage (compare the posterior *Uncx4.1*-negative domain in Fig. 2E,F, or the size of the *Msgn1* domain in Fig. 3G,H). Therefore, FGF signaling is not necessary to position the RA-responsive domain in the anterior PSM.

Oscillations of FGF signaling targets, such as *Spry2* in the mouse PSM, have recently implicated this pathway in the segmentation clock mechanism, and this pulse of FGF signaling occurs in phase with Notch signaling (Dequeant et al., 2006). However, in chick embryo cultures, short-term treatments with pharmacological inhibitors of FGF signaling or the MAPK pathway do not block oscillations of the Notch cyclic genes (Delfini et al., 2005; Dubrulle et al., 2001), and *Spry2* expression remains dynamic in the mouse Notch mutant for *RBPjk9* (also known as *Rbpj* –Mouse Genome Informatics) (Dequeant et al., 2006). This suggests that whereas NOTCH and FGF oscillate synchronously, their oscillations are controlled largely independently. To evaluate this further, we examined the expression of cyclic genes in *Fgfr1$^{f/f}$;T-Cre* mutant embryos. Prior to the 8-somite stage when FGF signaling is maintained in the posterior PSM of *Fgfr1$^{f/f}$;T-Cre* mutant embryos,

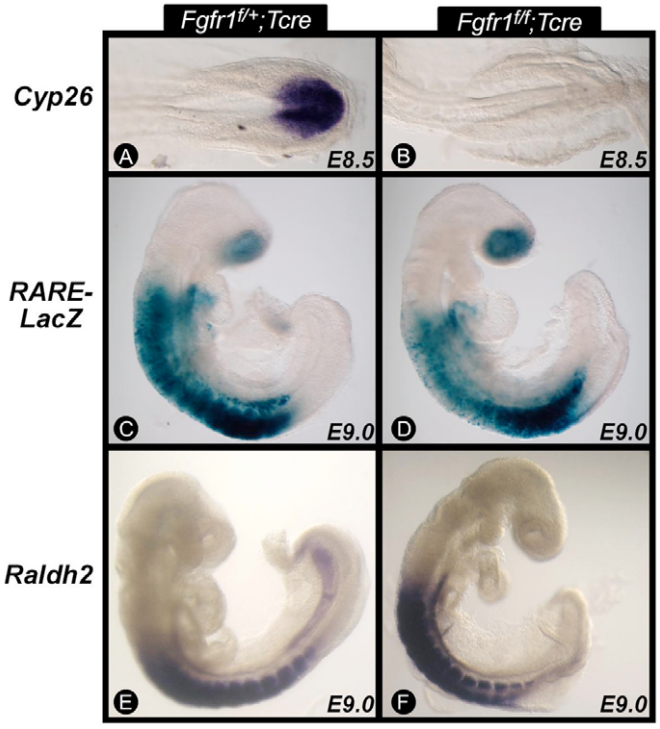

Fig. 5. FGF signaling is not sufficient to position the RA-responsive domain in the PSM. (**A**,**B**) *Cyp26* expression in the posterior region of the *Fgfr1$^{f/f}$;T-Cre* (B) mutant is downregulated compared with that in *Fgfr1$^{f/+}$;T-Cre* control (A) embryos. (**C**,**D**) There is a lack of significant change in RA activity, as detected by crossing to *RARE-lacZ* reporter mice, in *Fgfr1$^{f/f}$;T-Cre* mutant (D) compared with the *Fgfr1$^{f/+}$;T-Cre* control (C) embryos. (**E**,**F**) Expression of *Raldh2* is not significantly changed in the PSM of *Fgfr1$^{f/f}$;T-Cre* mutant embryos (F) compared with control *Fgfr1$^{f/+}$;T-Cre* (E) embryos.

the NOTCH cyclic gene *Lfng*, the WNT cyclic genes *Dkk1* and *Axin2*, as well as the FGF cyclic genes *Spry2* and *Snail1*, show different expression patterns, suggesting that the clock function is essentially normal (data not shown). However, in embryos with more than 10 somites, all cyclic genes show abnormal expression patterns (Fig. 6A-H). *Lfng* (n=15, Fig. 6B), intronic *Lfng* (n=4, data not shown) and *Spry2* (n=10, Fig. 6D) display an anterior-to-posterior expression gradient with no expression in the tail bud. *Axin2* (n=18, Fig. 6F), *Dkk1* (n=7, data not shown) and *Snail1* (n=4, Fig. 6H) have an opposite expression pattern, with strong staining in the tail bud but virtually no expression in the PSM. Disruption of the NOTCH cyclic gene oscillations is accompanied by abnormal expression in the PSM of several genes of the NOTCH pathway including *Dll1* (Fig. 3K,L), *Dll3* (Fig. 3O,P) and *Notch1* (Fig. 3M,N). Both *Notch1* and *Dll1* are upregulated in the tail bud and posterior PSM, while *Dll3* is severely downregulated, showing a faint 'salt-and-pepper' expression (Fig. 3O,P). Therefore, FGF signaling is required for oscillations of cyclic genes of the WNT, NOTCH and FGF pathway in the PSM.

Pharmacological inhibition of FGF signaling in mouse embryos disrupts Wnt and Notch oscillations with different kinetics

To further confirm the disruption of cyclic gene oscillations in the absence of FGF signaling, we cultured mouse tails in the presence of either the FGF receptor 1 inhibitor SU5402 (Mohammadi et al.,

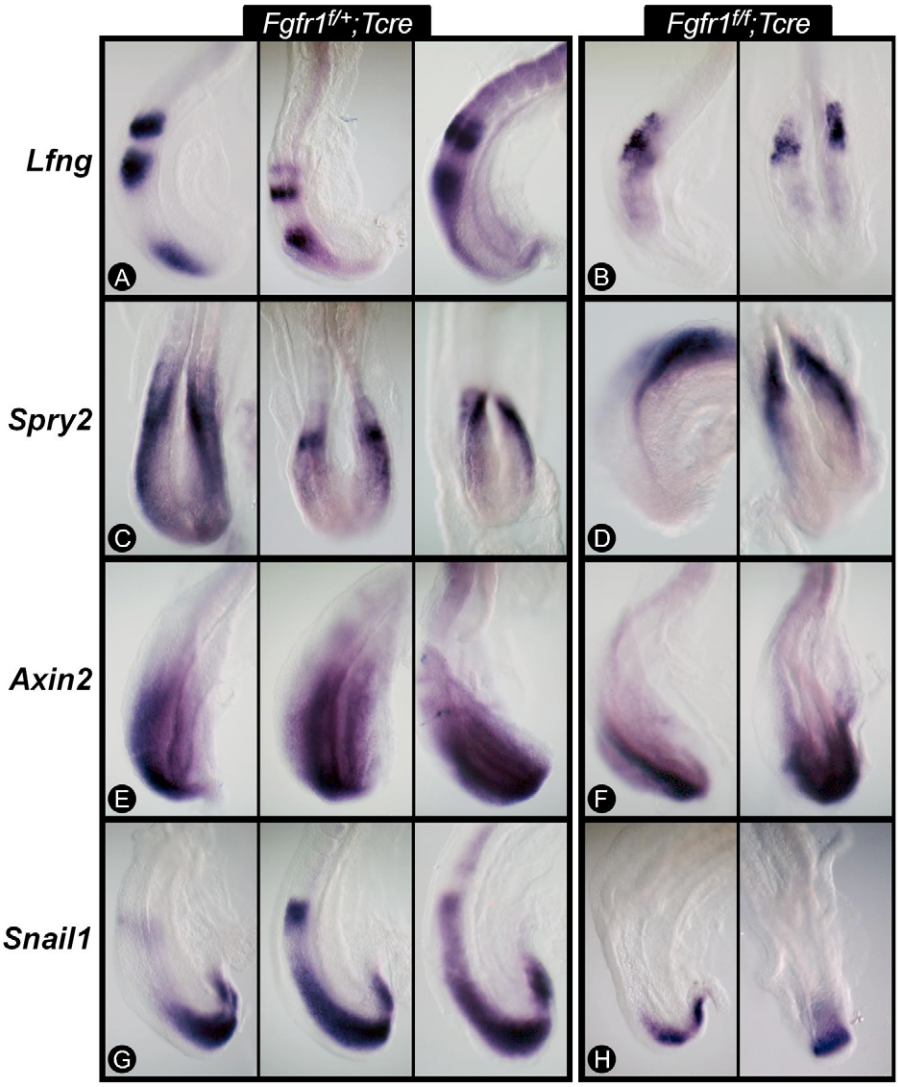

Fig. 6. Disruption of cyclic gene expression in the *Fgfr1$^{f/f}$;T-Cre* mutant embryos. (**A-H**) Comparison of expression of the cyclic genes of the Notch (*Lfng*), FGF (*Spry2, Snail1*) and Wnt (*Axin2*) signaling pathways at stages E8.75 (A-F) and E9.0 (G,H). All genes show dynamic expression in heterozygous *Fgfr1$^{f/+}$;T-Cre* control embryos (A,C,E,G). Oscillations in *Fgfr1$^{f/f}$;T-Cre* mutant embryos are lost (B,D,F,H). Lateral views are shown for *Fgfr1$^{f/+}$;T-Cre* in A,E,G and dorsal views are shown in C. For *Fgfr1$^{f/f}$;T-Cre* mutant (B,D,F,H), a lateral view is shown in the left panels, whereas dorsal views are shown in the right panels.

1997) or the MKK1 inhibitor U0126 (DeSilva et al., 1998) (which blocks ERK phosphorylation) and analyzed the dynamic expression of *Spry2, Axin2* and *Lfng* (Table 1 and data not shown). We used two different culture conditions (i.e. hanging drop culture in 10% FBS in DMEM-F12 or hanging drop culture in 50% rat serum in DMEM-F12) with E9.5 mouse tails (Correia and Conlon, 2000) and examined, by in situ hybridization, the expression of FGF target genes as a control for each batch of cultured embryos. As expected, the FGF target *Spry2* is rapidly downregulated in the posterior PSM after SU5402 or U0126 treatment for 2 hours, whereas control tails cultured in DMSO maintained dynamic expression patterns for *Spry2* (n=18, data not shown). Distinct patterns of *Axin2* were evident in DMSO-cultured control tails, but the expression of *Axin2* in the PSM of the treated embryos was downregulated after 2 hours in more than 80% of the explants, whereas it was always expressed in the tail bud (Table 1 and data not shown). This rapid downregulation of *Axin2* in the PSM, which occurs during the first oscillation cycle after treatment, suggests that *Axin2* might be directly regulated by FGF signaling through the MAPK pathway. Strikingly, a different situation was observed for *Lfng*. Whereas no significant change in expression was detected after 2 hours in culture, most embryos treated with SU5402 or U0126 began to show a similar pattern after 3 hours, a time corresponding to one clock oscillation period in these culture conditions (Table 1 and data not shown). This pattern was evident as a single stripe located in the anterior PSM and resembling phase III of the normal cycle (Pourquie and Tam, 2001) (data not shown). Therefore, blocking FGF signaling in vitro using pharmacological inhibitors disrupts the first cycle of *Axin2* oscillations but acts only after a one cycle delay on *Lfng* oscillations.

DISCUSSION

Here, we show that a conditional deletion of *Fgfr1*, the only FGF receptor expressed in the mouse PSM, blocks somite formation. Therefore, this provides a genetic demonstration for the role of FGF signaling in vertebrate segmentation. In the mutants, however, FGF signaling remains active during formation of the first somites that appear essentially normal (Fig. 2D, Fig. 7). This delay is somehow surprising because the *T-Cre* driver has been shown to be active from the earliest stages of gastrulation (Perantoni et al., 2005). The delayed progressive onset of the phenotypes observed could be explained by the stability of the *Fgfr1* transcript and protein. Following the formation of the first five somites or so, gradual downregulation of the FGF targets is observed in the PSM, indicating a progressive downregulation of the pathway activation. In the mutants, however, the first 10-13 somites appear essentially

Table 1. Summary of the expression of FGF target genes in tail cultures in the absence (DMSO control) and presence of either the FGFR1 inhibitor SU5402 or the MAPK inhibitor U0126

	Culture condition	Phase I	Phase II	Phase III	Phase inhibitor	*n*
Lfng						
2 h	DMSO	33	39	28		18
	U0126	26	39	35		23
	SU5402	8	33	58		12
3 h	DMSO	40	40	20		5
	SU5402	28	18	55		40
4 h	DMSO	33	33	33		15
	SU5402	10	20	70		40
6 h	DMSO	40	30	30		10
	SU5402	6	12	82		17
Axin2						
2 h	DMSO	33	33	33	0	21
	SU5402	0	5	10	85	20
3 h	DMSO	30	40	30	0	10
	SU5402	0	0	0	100	14
4 h	DMSO	33	33	33	0	3
	SU5402	0	0	0	100	9

Percentage of tails in Phases I, II and III are given for each combination at 2, 3, 4 and 6 hours. For *Axin2*, which shows an abnormal expression pattern after inhibitor treatment (data not shown), an additional column (Phase inhibitor) is introduced.

normal. In the mouse, the PSM contains around six presumptive somites (Tam, 1986), meaning that the precursors of somites 10-13 were already located in the posterior PSM when the downregulation of FGF signaling began. This suggests that enough FGF signaling was still available to allow proper specification of these somites. Posterior to somites 10-13, transient formation of a few larger irregular somites was observed (Fig. 2H), a phenotype similar to that observed in fish or chick following treatments with drugs blocking FGF signaling, such as SU5402 (Dubrulle et al., 2001; Sawada et al., 2001). Such a phenotype is predicted by the clock and wavefront model, since downregulating FGF signaling triggers a posterior shift of the wavefront, which is expected to lead to the formation of larger somites (Dubrulle and Pourquie, 2004a). Surprisingly, *Uncx4.1* whose expression is normally restricted to the posterior compartment of the somites, was sometimes found in the middle or in the anterior part of these larger somites, supporting the idea that rostrocaudal patterning can be uncoupled from segment formation (Nomura-Kitabayashi et al., 2002). No segments form posterior to the larger somites in mutant embryos, despite the continuous production of paraxial mesoderm from the tail bud. This paraxial mesoderm matures and differentiates into axial skeleton, but no somite boundaries form, although some coarse segmental pattern of the skeletal elements is, nevertheless, observed. This disruption of segmentation follows the level where arrest of the oscillations of the segmentation clock begins, further supporting the role of cyclic gene oscillations in the segmentation process (Fig. 6). Thus, our data provide genetic evidence for the role of FGF signaling in controlling the wavefront progression, a process involved in somite boundary positioning.

RALDH2, the RA biosynthetic enzyme, is expressed in the segmented region of the embryo and establishes an anterior-to-posterior signaling gradient that is involved in the control of cell differentiation and segmentation (Diez del Corral and Storey, 2004; Sirbu and Duester, 2006; Vermot et al., 2005). In the mouse, expression of the RA-signaling reporter *RARE-lacZ* is only detected in the anterior somites, suggesting that the RA signaling only acts early in the embryo in anterior somite precursors (Sirbu and Duester, 2006; Vermot et al., 2005). This is further supported by the fact that posterior somite formation in *Radlh2*-null mutants can be rescued by early RA treatment (Sirbu and Duester, 2006). However, these observations are difficult to reconcile with the fact that expression of *Raldh2* in the segmented region and of *Cyp26* in the tail bud extend all along the AP axis (Fujii et al., 1997; Niederreither et al., 1997). Moreover, a *Cyp26* null mutation in the mouse leads to axis truncation at the lumbar level, suggesting that RA plays a role in the formation of posterior somites as well (Sakai et al., 2001). In the chick embryo, FGF signaling has been shown to antagonize the RA gradient and to maintain the undifferentiated state of cells in the posterior part of the embryo throughout somitogenesis (Diez del Corral and Storey, 2004; Mathis et al., 2001; Vermot and Pourquie, 2005). Experiments in chick and frog have led to the proposal that in the PSM these mutually antagonistic gradients are necessary for the appropriate positioning of the determination front (Diez del Corral et al., 2003; Moreno and Kintner, 2004; Vermot and Pourquie, 2005). This hypothesis, however, is challenged by the observation that mouse *Raldh2* null mutants and vitamin A-deficient quail embryos (which cannot synthesize RA) form smaller, yet reasonably normal somites (Maden et al., 2000; Niederreither et al., 1999). Thus, in amniotes, RA

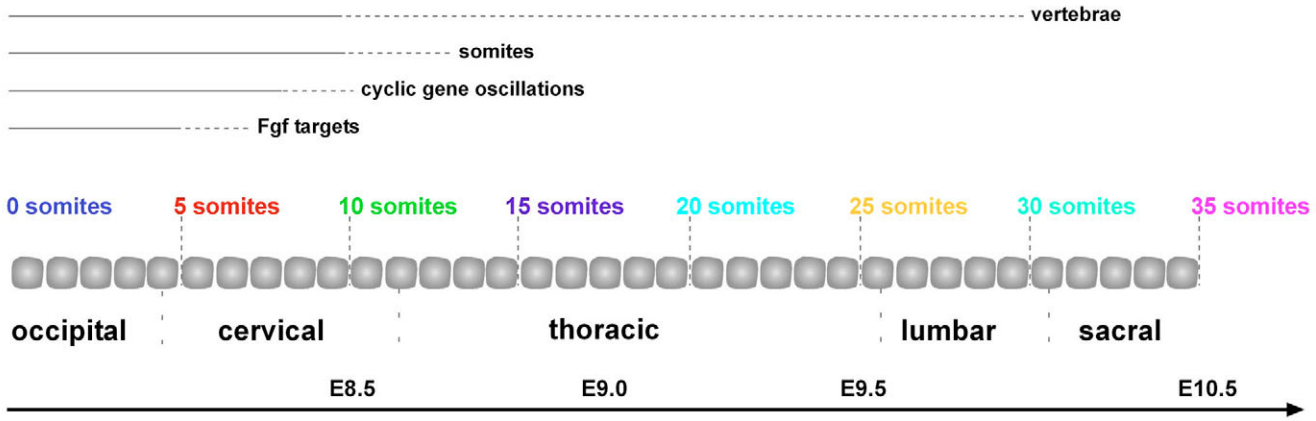

Fig. 7. Summary of the onset of the phenotypes observed in *Fgfr1$^{f/f}$;T-Cre* mutant embryos. FGF target genes become downregulated in the posterior PSM of *Fgfr1$^{f/f}$;T-Cre* mutant embryos at the 5- to 7-somite stage, followed by the arrest of cyclic gene expression between somites 8 and 10. Normal somites and corresponding vertebrae elements are observed up to somites 10 to 13; however, abnormal skeletal elements derived from paraxial mesoderm posterior to somite 13 were present.

signaling plays a role in refining the positioning of the determination front but is not critically required for boundary formation. Our results indicate that up to E9, the *Raldh2*- and the *RARE-lacZ*-positive domains in the PSM are not significantly extended posteriorly in *Fgfr1* conditional mutants despite the absence of the RA-degrading enzyme CYP26 in the posterior part of the embryo. This argues that in contrast to the situation in chick and frog, in the mouse FGF signaling antagonism is insufficient to explain the anterior positioning of the RA signaling domain (Diez del Corral et al., 2003; Moreno and Kintner, 2004). WNT signaling has also been shown to establish a posterior-to-anterior gradient that plays a role in the positioning of the determination front in the mouse (Aulehla et al., 2003). In the conditional mutants, *Wnt3a* (Fig. 3C,D) and its downstream targets *T* (Fig. 3E,F) and *Axin2* (Fig. 6E,F) are still expressed posteriorly, suggesting that WNT signaling is still active in the PSM. Thus, WNT signaling could act redundantly with FGF signaling to antagonize RA signaling in the PSM. Alternatively, the smaller somite size observed in *Raldh2* mutants has been proposed to result indirectly from an early antagonistic effect of RA on FGF signaling in the node and posterior neural plate (Sirbu and Duester, 2006). Such an effect is likely to be intact in the *Fgfr1* mutants, because the *T* promoter fragment does not drive expression in the node at these stages, and thus could account for the lack of effect on the positioning of the later RA domain seen in *Fgfr1* conditional mutants (Perantoni et al., 2005).

Oscillations of downstream targets of FGF signaling, such as *Spry2* or *Dusp6* (Dequeant et al., 2006), combined with our observations that FGF signaling is required for oscillations of cyclic genes of the WNT, NOTCH and FGF pathway in the PSM, provide evidence for a cyclic activation of the pathway in the PSM. On the other hand, graded distribution of the ligands and of the downstream effectors such as phosphorylated ERK (Delfini et al., 2005; Sawada et al., 2001) and AKT (Dubrulle and Pourquie, 2004b) shows that FGF signaling is also activated in a graded fashion along the PSM. A similar situation is also observed for WNT signaling which was shown to be periodically activated in the PSM and forms a signaling gradient in the tissue (Aulehla et al., 2003). Although at first glance these observations seem difficult to reconcile, several possible explanations can be envisioned to account for this situation. First, it could be that the pathway shows an overall graded yet periodic activation in the posterior PSM (Aulehla et al., 2003). These fluctuations could be sufficient to elicit periodic transcript production, but not to be detected biochemically using tools such as anti-phosphorylated ERK antibodies. We previously showed that phosphorylated ERK is extremely unstable in the mouse embryo PSM and hence, detecting small cyclic fluctuations might be technically very challenging (Delfini et al., 2005). Alternatively, it could be that FGF signaling is distributed uniformly in a graded fashion and is essentially required permissively for cyclic gene oscillations and its periodic transcription would be controlled independently of FGF signaling.

Oscillations of *Lfng*, *Spry2* and *Axin2* are also disrupted in cultures of mouse tails in the presence of pharmacological inhibitors of FGF signaling. In these experiments, the WNT cyclic gene *Axin2* and the FGF cyclic gene *Spry2* are rapidly downregulated in the PSM after inhibitor treatment, whereas *Lfng* expression continues to oscillate for one cycle. The observation that *Lfng* oscillations are halted in the *vestigial tail* mouse mutant led to the suggestion that in the mouse, the WNT pathway acts upstream of NOTCH oscillations (Aulehla et al., 2003). These data are therefore consistent with FGF indirectly controlling NOTCH oscillations via the WNT pathway. In summary, these data provide direct genetic evidence supporting the role of FGF signaling in the wavefront, which is involved in positioning somite boundaries in the PSM and in establishing a hierarchy in the NOTCH, WNT and FGF signaling pathways involved in the control of oscillatory expression of cyclic genes in the PSM.

We thank members of the Pourquié lab for discussions and comments, Stowers Institute Core Facilities, Joanne Chatfield for help on the manuscript and Silvia Esteban for artwork. This work was supported by Stowers Institute for Medical Research. O.P. is a Howard Hughes Medical Investigator.

References

Aulehla, A., Wehrle, C., Brand-Saberi, B., Kemler, R., Gossler, A., Kanzler, B. and Herrmann, B. G. (2003). Wnt3a plays a major role in the segmentation clock controlling somitogenesis. *Dev. Cell* **4**, 395-406.

Chotteau-Lelievre, A., Dolle, P., Peronne, V., Coutte, L., de Launoit, Y. and Desbiens, X. (2001). Expression patterns of the Ets transcription factors from the PEA3 group during early stages of mouse development. *Mech. Dev.* **108**, 191-195.

Cooke, J. and Zeeman, E. C. (1976). A clock and wavefront model for control of the number of repeated structures during animal morphogenesis. *J. Theor. Biol.* **58**, 455-476.

Correia, K. M. and Conlon, R. A. (2000). Surface ectoderm is necessary for the morphogenesis of somites. *Mech. Dev.* **91**, 19-30.

Crossley, P. H. and Martin, G. R. (1995). The mouse *Fgf8* gene encodes a family of polypeptides and is expressed in regions that direct outgrowth and patterning in the developing embryo. *Development* **121**, 439-451.

Delfini, M. C., Dubrulle, J., Malapert, P., Chal, J. and Pourquie, O. (2005). Control of the segmentation process by graded MAPK/ERK activation in the chick embryo. *Proc. Natl. Acad. Sci. USA* **102**, 11343-11348.

Deng, C. X., Wynshaw-Boris, A., Shen, M. M., Daugherty, C., Ornitz, D. M. and Leder, P. (1994). Murine FGFR-1 is required for early postimplantation growth and axial organization. *Genes Dev.* **8**, 3045-3057.

Dequeant, M. L., Glynn, E., Gaudenz, K., Wahl, M., Chen, J., Mushegian, A. and Pourquie, O. (2006). A complex oscillating network of signaling genes underlies the mouse segmentation clock. *Science* **314**, 1595-1598.

DeSilva, D. R., Jones, E. A., Favata, M. F., Jaffee, B. D., Magolda, R. L., Trzaskos, J. M. and Scherle, P. A. (1998). Inhibition of mitogen-activated protein kinase kinase blocks T cell proliferation but does not induce or prevent anergy. *J. Immunol.* **160**, 4175-4181.

Diez del Corral, R. and Storey, K. G. (2004). Opposing FGF and retinoid pathways: a signalling switch that controls differentiation and patterning onset in the extending vertebrate body axis. *BioEssays* **26**, 857-869.

Diez del Corral, R., Olivera-Martinez, I., Goriely, A., Gale, E., Maden, M. and Storey, K. (2003). Opposing FGF and retinoid pathways control ventral neural pattern, neuronal differentiation, and segmentation during body axis extension. *Neuron* **40**, 65-79.

Dubrulle, J. and Pourquie, O. (2004a). Coupling segmentation to axis formation. *Development* **131**, 5783-5793.

Dubrulle, J. and Pourquie, O. (2004b). fgf8 mRNA decay establishes a gradient that couples axial elongation to patterning in the vertebrate embryo. *Nature* **427**, 419-422.

Dubrulle, J., McGrew, M. J. and Pourquie, O. (2001). FGF signaling controls somite boundary position and regulates segmentation clock control of spatiotemporal Hox gene activation. *Cell* **106**, 219-232.

Fujii, H., Sato, T., Kaneko, S., Gotoh, O., Fujii-Kuriyama, Y., Osawa, K., Kato, S. and Hamada, H. (1997). Metabolic inactivation of retinoic acid by a novel P450 differentially expressed in developing mouse embryos. *EMBO J.* **16**, 4163-4173.

Henrique, D., Adam, J., Myat, A., Chitnis, A., Lewis, J. and Ish-Horowicz, D. (1995). Expression of a Delta homologue in prospective neurons in the chick. *Nature* **375**, 787-790.

Kessel, M., Balling, R. and Gruss, P. (1990). Variations of cervical vertebrae after expression of a Hox-1.1 transgene in mice. *Cell* **61**, 301-308.

Maden, M., Graham, A., Zile, M. and Gale, E. (2000). Abnormalities of somite development in the absence of retinoic acid. *Int. J. Dev. Biol.* **44**, 151-159.

Mansour, S. L., Goddard, J. M. and Capecchi, M. R. (1993). Mice homozygous for a targeted disruption of the proto-oncogene int-2 have developmental defects in the tail and inner ear. *Development* **117**, 13-28.

Mansouri, A., Yokota, Y., Wehr, R., Copeland, N. G., Jenkins, N. A. and Gruss, P. (1997). Paired-related murine homeobox gene expressed in the developing sclerotome, kidney, and nervous system. *Dev. Dyn.* **210**, 53-65.

Maruoka, Y., Ohbayashi, N., Hoshikawa, M., Itoh, N., Hogan, B. L. and Furuta, Y. (1998). Comparison of the expression of three highly related genes, Fgf8, Fgf17 and Fgf18, in the mouse embryo. *Mech. Dev.* **74**, 175-177.

Mathis, L., Kulesa, P. M. and Fraser, S. E. (2001). FGF receptor signalling is required to maintain neural progenitors during Hensen's node progression. *Nat. Cell Biol.* **3**, 559-566.

Mohammadi, M., McMahon, G., Sun, L., Tang, C., Hirth, P., Yeh, B. K., Hubbard, S. R. and Schlessinger, J. (1997). Structures of the tyrosine kinase

domain of fibroblast growth factor receptor in complex with inhibitors. *Science* **276**, 955-960.
Moreno, T. A. and Kintner, C. (2004). Regulation of segmental patterning by retinoic acid signaling during Xenopus somitogenesis. *Dev. Cell* **6**, 205-218.
Niederreither, K., McCaffery, P., Drager, U. C., Chambon, P. and Dolle, P. (1997). Restricted expression and retinoic acid-induced downregulation of the retinaldehyde dehydrogenase type 2 (RALDH-2) gene during mouse development. *Mech. Dev.* **62**, 67-78.
Niederreither, K., Subbarayan, V., Dolle, P. and Chambon, P. (1999). Embryonic retinoic acid synthesis is essential for early mouse post-implantation development. *Nat. Genet.* **21**, 444-448.
Niswander, L. and Martin, G. R. (1992). Fgf-4 expression during gastrulation, myogenesis, limb and tooth development in the mouse. *Development* **114**, 755-768.
Nomura-Kitabayashi, A., Takahashi, Y., Kitajima, S., Inoue, T., Takeda, H. and Saga, Y. (2002). Hypomorphic *Mesp* allele distinguishes establishment of rostrocaudal polarity and segment border formation in somitogenesis. *Development* **129**, 2473-2481.
Palmeirim, I., Henrique, D., Ish-Horowicz, D. and Pourquié, O. (1997). Avian hairy gene expression identifies a molecular clock linked to vertebrate segmentation and somitogenesiss. *Cell* **91**, 639-648.
Perantoni, A. O., Timofeeva, O., Naillat, F., Richman, C., Pajni-Underwood, S., Wilson, C., Vainio, S., Dove, L. F. and Lewandoski, M. (2005). Inactivation of FGF8 in early mesoderm reveals an essential role in kidney development. *Development* **132**, 3859-3871.
Pourquie, O. (2003). The segmentation clock: converting embryonic time into spatial pattern. *Science* **301**, 328-330.
Pourquie, O. and Tam, P. P. (2001). A nomenclature for prospective somites and phases of cyclic gene expression in the presomitic mesoderm. *Dev. Cell* **1**, 619-620.
Rossant, J., Zirngibl, R., Cado, D., Shago, M. and Giguere, V. (1991). Expression of a retinoic acid response element-hsplacZ transgene defines specific domains of transcriptional activity during mouse embryogenesis. *Genes Dev.* **5**, 1333-1344.
Sakai, Y., Meno, C., Fujii, H., Nishino, J., Shiratori, H., Saijoh, Y., Rossant, J. and Hamada, H. (2001). The retinoic acid-inactivating enzyme CYP26 is essential for establishing an uneven distribution of retinoic acid along the anterio-posterior axis within the mouse embryo. *Genes Dev.* **15**, 213-225.
Sawada, A., Shinya, M., Jiang, Y. J., Kawakami, A., Kuroiwa, A. and Takeda, H. (2001). Fgf/MAPK signalling is a crucial positional cue in somite boundary formation. *Development* **128**, 4873-4880.
Sirbu, I. O. and Duester, G. (2006). Retinoic-acid signalling in node ectoderm and posterior neural plate directs left-right patterning of somitic mesoderm. *Nat. Cell Biol.* **8**, 271-277.
Sun, X., Meyers, E. N., Lewandoski, M. and Martin, G. R. (1999). Targeted disruption of Fgf8 causes failure of cell migration in the gastrulating mouse embryo. *Genes Dev.* **13**, 1834-1846.
Tam, P. P. (1986). A study of the pattern of prospective somites in the presomitic mesoderm of mouse embryos. *J. Embryol. Exp. Morphol.* **92**, 269-285.
Verheyden, J. M., Lewandoski, M., Deng, C., Harfe, B. D. and Sun, X. (2005). Conditional inactivation of *Fgfr1* in mouse defines its role in limb bud establishment, outgrowth and digit patterning. *Development* **132**, 4235-4245.
Vermot, J. and Pourquie, O. (2005). Retinoic acid coordinates somitogenesis and left-right patterning in vertebrate embryos. *Nature* **435**, 215-220.
Vermot, J., Llamas, J. G., Fraulob, V., Niederreither, K., Chambon, P. and Dolle, P. (2005). Retinoic acid controls the bilateral symmetry of somite formation in the mouse embryo. *Science* **308**, 563-566.
Xu, X., Qiao, W., Li, C. and Deng, C. X. (2002). Generation of Fgfr1 conditional knockout mice. *Genesis* **32**, 85-86.